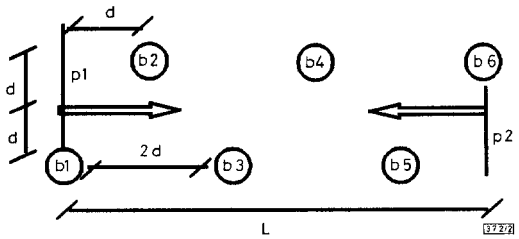

Fig. 2 *Mobiles travelling in opposite direction and crossing at 2.5km from b1*

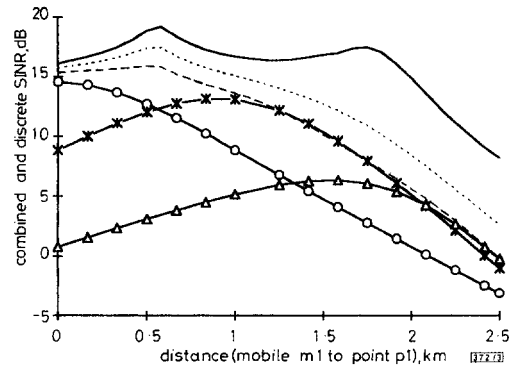

Fig. 3 *Overall SINR compared with individual SINR of each cell*

—○— cell 1 —✳— cell 2 —△— cell 3
– – – lower SINR —— upper SINR - - - - mean SINR

transmit with the same power and frequency and depart with the same velocity, in a linear direction. The distance from $p1$ to $p2$ is L = 5km. The effects of the Doppler frequency shift on the estimate of the SINR are not considered. All the other impairments (nonlinearities of receiving filters, background noise, frequency offset, etc.) are modelled as Gaussian with normalised $SINR$ = 15 dB, measured at $b1$ as the initial condition. The SINR parameter can be estimated in a practical way as given by [6], if the system uses constant-modulus modulation (e.g. $\pi/4$ QPSK, GMSK, etc.). For the phase combination, any method suitable for antenna arrays [8] can be used. Here, this combination is performed in three ways: (*a*) the wanted signal and the interference from all cells are combined in phase; (*b*) the wanted signal is combined in phase whilst the interference is combined with opposite phases (neutralising); (*c*) the total interference power is the sum of individual interference mean powers (independent interferers). By doing so, the overall SINR (after combination) is bounded by two extreme cases. The first case (item *a*) can be seen as a lower bound (no other combination gives a lower SINR). The second case (item *b*) is an upper bound. The third case is a more realistic average. They are plotted in Fig. 3 as the mobiles move, getting closer. Fig. 3 also shows the SINR in each cell ($b1$, $b2$ and $b3$) alone. From the Figure it is clear that the overall quality of combined signals is always better than, or at least equal to, that of a cell alone. This reduces the need for handover along cluster borders and permits frequency reuse inside a cluster.

Conclusions: Base station macro-diversity combining has been presented for implementing a mobile cellular system. In this scheme, a cell identifies simply with a base station. The signal from a mobile is combined by all cells in a cluster. This provides better protection against interference and diminishes the necessity of handover alongside cluster borders. There is no predetermined set of base stations managing one call. A cell participates in the control over a mobile as long as it perceives a good reception. Unless the signal quality drops below a minimum standard, there is no need for handover, disregarding the location of the mobile. For those reasons, frequency reuse is allowed inside a cluster. We have obtained the overall SINR gain of the combining method over a diversity switching scheme, but without considering fading channels because the aim of this work is to introduce a combining system concept. If fading channels are considered, a gain over any switching technique (as far as outage probability is concerned) should also be obtained.

Acknowledgment: The author A.L. Brandão is supported by the Coordenação de Aperfeiçoamento de Pessoal de Nível Superior, CAPES, Brazil.

17 November 1994
Electronics Letters Online No: 19950072

A.L. Brandão, L.B. Lopes and D.C. McLernon (*Department of Electronic & Electrical Engineering, The University of Leeds, Leeds LS2 9JT, United Kingdom*)

References

1 CHIA, S.T.S.: 'Cellular structure and handover algorithms for a third generation mobile system', *BT Technol. J.*, 1993, **11**, (1), pp. 111–116
2 TEKINAY, S., and JABBARI, B.: 'Handover and channel assignment in mobile cellular networks', *IEEE Commun. Mag.*, 1991, **29**, (11), pp. 42–46
3 BERNHARDT, R.C.: 'Macroscopic diversity in frequency reuse radio systems', *IEEE J. Sel. Areas Commun.*, 1987, **SAC-5**, (5), pp. 862–870
4 KUCAR, A.D.: 'Mobile radio: an overview', *IEEE Commun. Mag.*, 1991, **29**, (11), pp. 73–85
5 JAKES, W.C.: 'Microwave mobile communications' (John Wiley & Sons, New York, 1974), Chap. 5, pp. 377–387
6 BRANDÃO, A.L., LOPES, L.B., and MCLERNON, D.C.: 'In service monitoring of multipath delay and cochannel interference for indoor mobile communications systems'. IEEE Int. Conf. on Communications, ICC'94, New Orleans, 1994, Vol. 2, pp. 1458–1462
7 HATA, M.: 'Empirical formula for propagation loss in land-mobile radio services', *IEEE Trans.*, 1980, **VT-29**, (3), pp. 317–325
8 WINTERS, J.H.: 'Optimum combining in digital mobile radio with cochannel interference', *IEEE J. Sel. Areas Commun.*, 1984, **SAC-2**, (4), pp. 528–539

Buffer occupancy in ATM switches with single hot spot

M. Saleh and M. Atiquzzaman

Indexing terms: Asynchronous transfer mode, Digital communication systems

ATM switches based on shared buffering are known to have better buffer utilisation. However, in the presence of hot spot traffic, buffers become monopolised in favour of hot output. In the Letter, we present the effect of buffer monopoly in a shared buffer switch and discuss the solutions to this phenomenon.

Introduction: A multistage ATM switch consists of a number of stages of small switching elements (SEs) which are interconnected by a permutation function. A group of multistage switches, known as Delta switches, consists of n stages of $d \times d$ SEs, where $d^n = N$ is the number of inputs or outputs of the switch. In a shared buffer Delta switch, there are B buffer spaces in each SE which are shared among all of the inlets and outlets of the SE, i.e. a cell at any inlet may be placed in any buffer slot, and from there it can be destined to any outlet of the SE. Unlike input buffering, there is no head of line blocking in shared buffer switches, and total buffer utilisation is better than output buffering. However, in the presence of hot spot traffic, the hot traffic saturates the buffers in the SE rapidly, which results in degradation in the performance of the switch.

In this Letter we study the distribution of buffer length, defined as buffer occupancy, at different stages of Delta switches in the presence of hot spot traffic.

Assumptions and notation: The following assumptions are made regarding the switch and its operation:

A backpressure mechanism with global flow control ensures that no cell is lost inside the switch. The process of forwarding and accepting cells in each SE is virtually accomplished in two phases. In the forward phase, depending on the state of the SE and its downstream SEs, a number of cells leave the SE. In the receive phase, the cells offered from upstream SEs are placed in the buffers.

Hot spot traffic is assumed. To formulate the single hot spot traffic mathematically, the probability of a cell arriving at a switch input and being destined to the hot output (p_h) or to any single one of the $N-1$ cold outputs (p_c) is given by:

$$p_h = \rho\left(f_h + \frac{1-f_h}{N}\right) \quad p_c = \rho\left(\frac{1-f_h}{N}\right)$$

$$p_h + (N-1)p_c = \rho$$

where f_h is the fraction of the traffic destined to the hot output of the switch.

The reader is referred to [1] for additional assumptions regarding the modelling of the shared-buffer Delta switch.

We model each SE by a Markov chain representing the distribution of the hot and cold cells stored in the B buffers of the SE. The state of an SE is represented by a tuple (h, c), where h is the number of cells destined to the hot outlet of the SE and c is the number of cells destined to the other $d-1$ cold outlets of the SE. We label the hot switch at any stage as a type 1 SE. An SE is of type i if it is fed by a type $i-1$ SE in the previous stage [2]. .

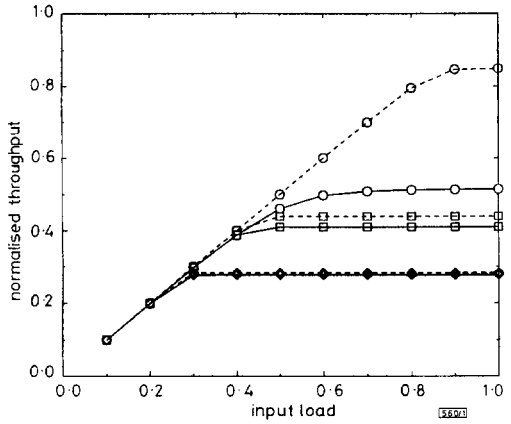

Fig. 1 *Normalised throughput against* ρ

$N = 256$, $d = 2$
○——○ $h = 0.0$, $B = 2$
□——□ $h = 0.005$, $B = 2$
◇——◇ $h = 0.01$, $B = 2$
○- - -○ $h = 0.0$, $B = 6$
□- - -□ $h = 0.005$, $B = 6$
◇- - -◇ $h = 0.01$, $B = 6$

The following notation will be used in the model:

$\pi_{i,r}(h1,c1)$: Steady-state probability that a type r SE at stage i is in state $(h1, c1)$.

$\pi_{i,r}(h1, c1, h3, c3)$: Steady-state probability that a type r SE at stage i is in state $(h3, c3)$ at the beginning of the receive phase, given that it was in state $(h1, c1)$ at the beginning of the forward phase, where $h1 \geq h3$ and $c1 \geq c3$.

$\sigma_{i,r}(h3, c3, h2, c2)$: Steady-state probability that a type r SE at stage i is in state $(h2, c2)$ at the end of the receive phase, given that it was in state $(h3, c3)$ at the beginning of the receive phase, where $h3 \leq h2$ and $c3 \leq c2$.

$\tilde{\pi}_{i,r}(h3, c3)$: Steady-state probability that a type r SE at stage i is in state $(h3, c3)$ at the beginning of the receive phase.

Hot spot model: In a steady-state condition, the Markov chain model of any $\pi_{i,r}$ tuple can be described as

$$\pi_{i,r}(h2,c2) = \sum_{h3=0}^{B}\sum_{c3=0}^{B-h3} \tilde{\pi}_{i,r}(h3,c3)\sigma_{i,r}(h3,c3,h2,c2)$$

$$\tilde{\pi}_{i,r}(h3,c3) = \sum_{h1=0}^{B}\sum_{c1=0}^{B-h1} \pi_{i,r}(h1,c1)\tau_{i,r}(h1,c1,h3,c3) \quad (1)$$

where B is the total buffer space in an SE.

The average throughput of an SE of type r in stage i is

$$\lambda_{i,r,av} = \sum_{h1=1}^{B}\sum_{c1=0}^{B-h1} \pi_{i,r}(h1,c1)\sum_{c3=0}^{c1}\tau_{i,r}(h1,c1,h1-1,c3) + \sum_{c1=1}^{B}\sum_{h1=0}^{B-c1}\pi_{i,r}(h1,c1)\sum_{h3=0}^{h1}\sum_{c3=\max(0,c1-d)}^{c1}(c1-c3)\tau_{i,r}(h1,c1,h3,c3) \quad (2)$$

The average throughput of a stage i is given by

$$\Lambda_i = d^{k-i}\left[\lambda_{i,1,av} + (d-1)\sum_{r=2}^{i}\lambda_{i,r,av}d^{r-2}\right] \quad (3)$$

Eqn. 3 applies to all of the stages, including the first stage, where Σ becomes irrelevant.

The expected value of the length of hot and cold virtual queues are obtained by

$$L_{i,r,hot} = \sum_{h=0}^{B}\sum_{c=0}^{B-h} h\pi_{i,r}(h,c) \quad (4)$$

$$L_{i,r,cold} = \frac{1}{d-1}\sum_{h=0}^{B}\sum_{c=0}^{B-h} c\pi_{i,r}(h,c) \quad (5)$$

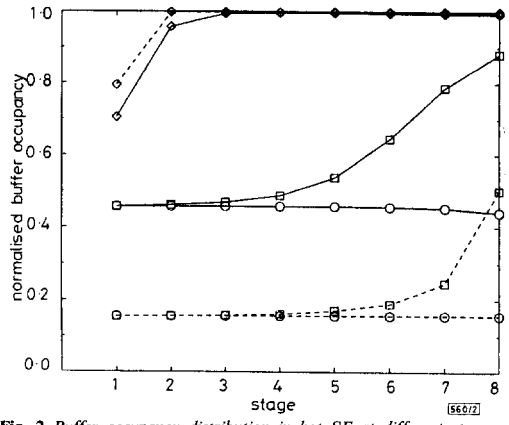

Fig. 2 *Buffer occupancy distribution in hot SE at different stages of Delta switch*

$N = 256$, $d = 2$, and $\rho = 0.4$
○——○ $h = 0.0$, $B = 2$
□——□ $h = 0.005$, $B = 2$
◇——◇ $h = 0.01$, $B = 2$
○- - -○ $h = 0.0$, $B = 6$
□- - -□ $h = 0.005$, $B = 6$
◇- - -◇ $h = 0.01$, $B = 6$

Numerical results: Fig. 1 illustrates the impact of hot spot traffic on the throughput of shared buffer switches for $N = 256$ and $d = 2$. The throughput of a shared buffer switch is degraded more when the B/d ratio increases. Fig. 2 shows the fraction of occupied buffers in the presence of hot spot traffic for the same switch and SE size as in Fig. 1, and for input load $\rho = 0.4$. As expected, under uniform traffic pattern and low input load, the distribution of buffer occupancy is almost constant in all of the stages. However, by the introduction of hot traffic, buffers in the hot SEs start to saturate. Saturation starts from the last stage, and affects predecessor stages in turn. For the given switch size and SE size, increasing the hot spot ratio to only 1% will saturate all but the

first stage for an input load of as low as 0.4. Increasing the buffer size has little effect on improving the throughput of the switch, since the buffer monopoly hinders the hot SEs from forwarding a reasonable traffic to their successor hot and cold SEs, and connected outputs thereafter. Although not shown here, there is the same trend of buffer occupancy when ρ increases, except that under uniform traffic the first stage has the highest buffer occupancy, and the occupancy decreases as the stage number increases

Conclusion: Although, under uniform traffic, buffers in a shared-buffer Delta switch are used more efficiently, free choice of buffer slot for any incoming cell at an SE causes significant congestion in the presence of hot spot traffic. This effect can be alleviated by using an additional control mechanism to limit the number of cells which are destined to the hot output of an SE. For example, it is possible to limit the hot traffic to 50% of total capacity of an SE. It is also possible to select different limits of hot traffic at different stages, since, depending on the stage, different numbers of outputs are affected by a congested hot SE. The selection of an optimum hot traffic limit at a given hot SE may be studied as an extension to this work.

5 December 1994
Electronics Letters Online No: 19950052

M. Saleh and M. Atiquzzaman (*Department of Computer Science and Computer Engineering, La Trobe University, Melbourne 3083, Australia*)

References

1 TURNER, J.S.: 'Queueing analysis of buffered switching networks', *IEEE Trans.*, 1993, **COM-41**, (2), pp. 412–420
2 ATIQUZZAMAN, M., and AKHTAR, M.S.: 'Effect of non-uniform traffic on the performance of unbuffered multistage interconnection networks', *IEE Proc. E*, 1994, **141**, (3), pp. 169–176

Journal code:- EL
Article production number:- 45560
Classification:- Communications & signal processing

Combined algorithm for pitch detection of speech signals

M.E. Hernández-Diaz Huici and J.V. Lorenzo Ginori

Indexing terms: Speech analysis and processing, Speech recognition

A new short-term pitch detection algorithm is reported, whose main features are good robustness in noisy environments, an accuracy which approximates that of superresolution integer algorithm, and reduced computational cost. Complete information regarding algorithm implementation is given, and experimental results for pitch contour extraction are shown.

Introduction: The remarkable advances in speech processing in the past two decades have led to the development of several pitch detection algorithms (PDAs). Many of them have been summarised and discussed by Hess [1] and Rabiner *et al.* [2]. The main features in characterisation and performance evaluation of PDAs are voiced/unvoiced decision error rate, fine and coarse pitch error, noise immunity and computational efficiency, each algorithm revealing some balance between these aspects. In this Letter the authors describe a new combined pitch detection algorithm (CPDA), having good accuracy, high noise immunity and low computational cost. The CPDA has a multichannel structure that combines the features of three different PDAs in a convenient way to reduce the computational burden and to improve reliability.

Combined pitch detection algorithm: The combined pitch detection algorithm has a three-channel structure, in which the input signal is previously processed by a digital bandpass filter and then processed in parallel by the three pitch detectors, as Fig. 1 shows.

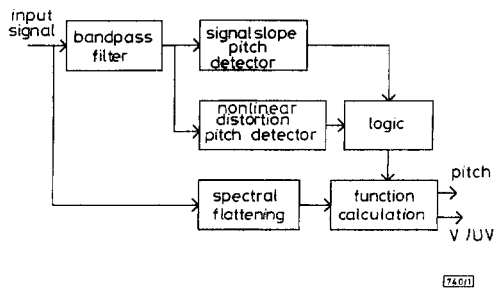

Fig. 1 *Block diagram of combined pitch detector algorithm*

The first one is a slope detector that locates the waveform peaks by means of minimum-maximum-minimum and associate slopes sequence detection, following the approaches of Jovanovic [3] and Gold and Rabiner [4].

The second pitch detector emphasises the greatest amplitude signal peaks by means of an exponential distortion given by

$$s_d(n) = \text{sign}[s(n)] \exp[K|s(n)|] \qquad (1)$$

where $K = 0.0162$ is an empirically calculated coefficient. The signal distorted in this way exhibits noticeable peaks spaced one pitch period away for voiced signal frames. It was found that this kind of distortion also produces some degree of spectral flattening.

Both the first and second algorithms simultaneously detect voicing for the signal frame by zero-crossing calculations and detectors' logic.

The third detector algorithm is based on the similarity model introduced by Medan *et al.* [5], taking into account the following changes:

(a) Centre clipping is used as a spectral flattening technique to reduce the formant structure effects, thus allowing the crosscorrelation function between adjacent signal windows to have a maximum for pitch period window duration.

(b) The correlation function is substituted by the function

$$\rho_n = \sum_{i=1}^{n} |x_i - y_i| \Big/ \sum_{i=1}^{n} |x_i| + |y_i| \qquad (2)$$

where n is the window length. This function, based on the AMDF function [6], is normalised to $0 \le \rho_n \le 1$, and it exhibits a deep null when n is the integer pitch, and local minima for multiples of n.

A logic is used to select the values of n_p for which it is possible to achieve further computational cost reduction in calculating ρ_n, in the following way:

(a) If the pitch estimates n_{p1} and n_{p2} from the first two detectors are equivalent or one of them is equal to zero (e.g. at least one estimate has been calculated), ρ_n is calculated for $n = n_{pe}/2$, n_{pe} and $2n_{pe}$. As soon as ρ_n is below some threshold (0.3 in this case), n_{pe} is taken as the integer pitch value and ρ_n is not calculated for the remaining values of n.

(b) If the first two pitch estimates n_{p1} and n_{p2} differ, ρ_n is calculated for $n_{p1} - 3 \le n \le n_{p2} + 3$.

The calculations are stopped when the minimum is detected and the corresponding value of n is taken as the pitch value.

Experimental results: The CPDA behaviour was evaluated following the approach of Rabiner *et al.* [2] for a representative speech signal database.

Table 1: Fine errors standard deviation

Speaker/method	Super-resolution	Auto-correlation	*DWS*	*CPDA*
Male 1	2.415	2.046	3.948	2.952
Male 2	2.428	2.019	4.220	2.497
Female	2.006	1.091	3.985	1.986